Electronic Supplementary Material (ESI) for Journal of Materials Chemistry C.

Supporting Information

Exploring the Effects of Interfacial Carrier Transport Layers on Device Performance and Optoelectronic Properties of Planar Perovskite Solar Cells

Dhruba B. Khadka,[†]* Yasuhiro Shirai,[†]* Masatoshi Yanagida,[†] James W. Ryan,[†‡] and Kenjiro Miyano[†]

[†] Global Research Center for Environment and Energy based on Nanomaterials Science (GREEN), National Institute for Materials Science (NIMS), 1-1 Namiki, Tsukuba, Ibaraki 305-0044, Japan.

[‡] International Center for Young Scientists (ICYS), National Institute for Materials Science (NIMS), 1-1 Namiki, Tsukuba, Ibaraki 305-0044, Japan.

Corresponding Authors

*E-mail:

KHADKA.B.Dhruba@nims.go.jp

SHIRAI.Yasuhiro@nims.go.jp

Table and Figures

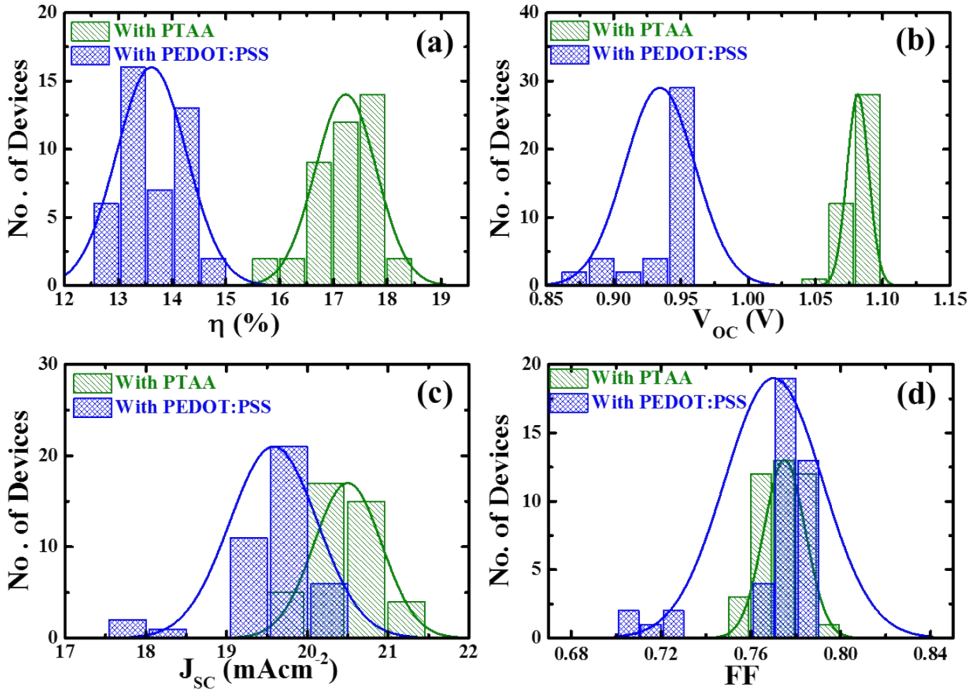

Figure S1. Statistical summary of performance of perovskite devices with PTAA and PEDOT:PSS as HTL. Histogram of device parameters: (a) efficiency (η), (b) V_{OC} , (c) J_{SC}, (d) FF of 40 devices fabricated 3 different batches.

Table S1. Statistics of respective device parameters. Avg: average, Max: maximum, Min: minimum, and Std: standard deviation.

Statistics of devices	With PTAA				With PEDOT:PSS			
	J_{SC} (mAcm^{-2})	V_{OC} (V)	FF	η (%)	J_{SC} (mAcm^{-2})	V_{OC} (V)	FF	η (%)
Avg	20.50	1.08	0.77	17.23	19.344	0.93	0.76	13.66
Max	21.02	1.09	0.79	18.07	20.22	0.95	0.78	14.53
Min	19.61	1.06	0.75	15.78	17.52	0.84	0.68	12.56
Std	0.42	0.01	0.01	0.57	0.64	0.03	0.03	0.61

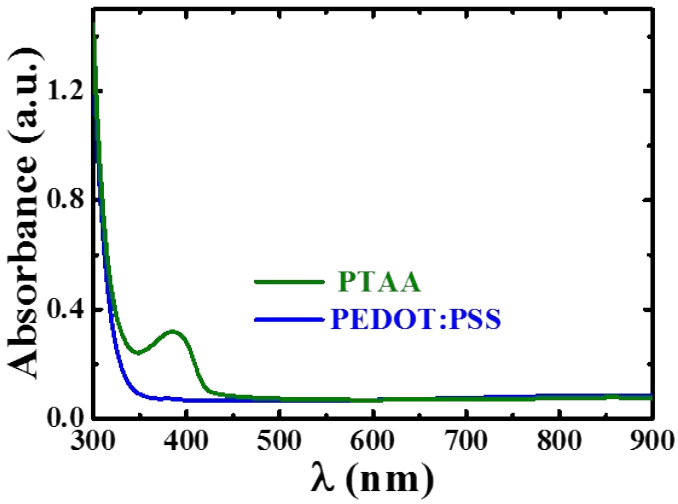

Figure S2. Absorption spectra of HTLs (PTAA and PEDOT:PSS).

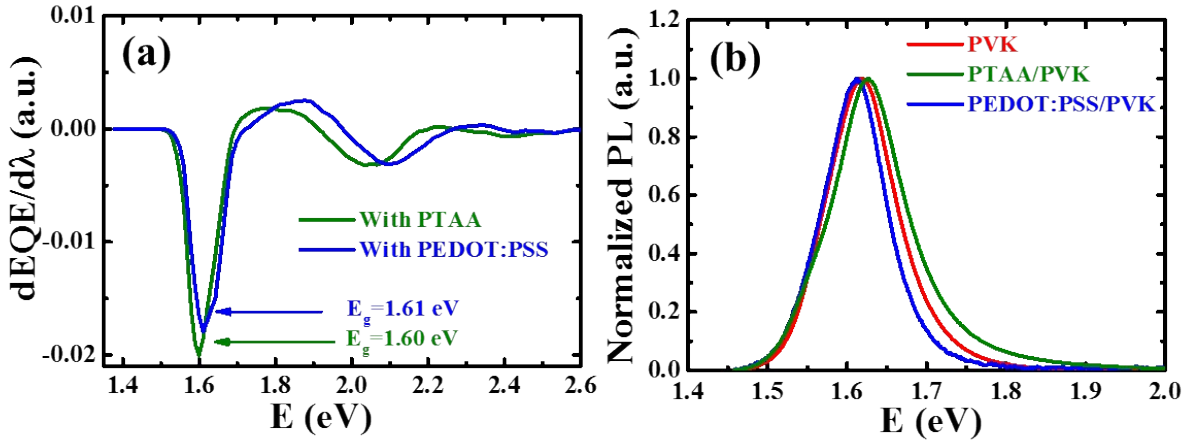

Figure S3. Estimation of band gap energy (E_g) of perovskite films from EQE data of respective devices (a). Normalized Photoluminance (PL) spectra of perovskite (PVK) films and PVK on grown PTAA and PEDOT:PSS with characteristics PL peak at 1.6 eV. It is good agreement to the band gap energy of perovskite layer estimated from EQE response.

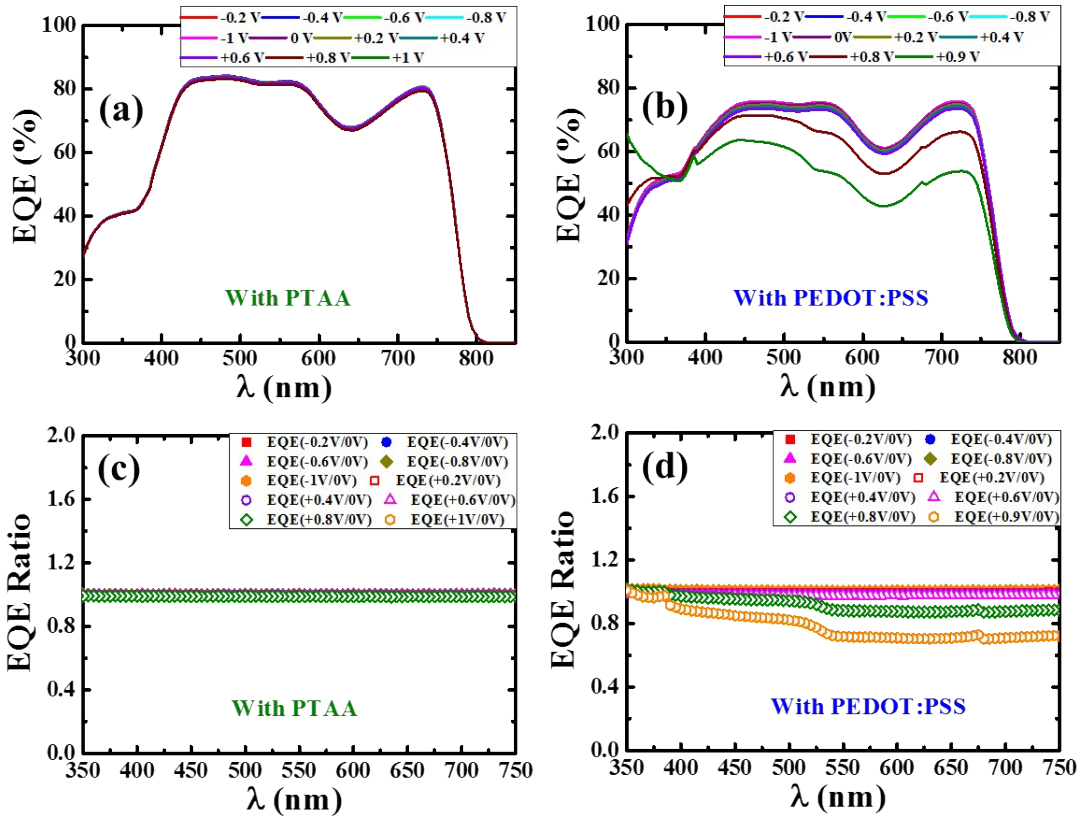

Figure S4. EQE spectra of devices measured under different bias voltage (a,b) and EQE ratio with respect to EQE at 0V bias (c,d).

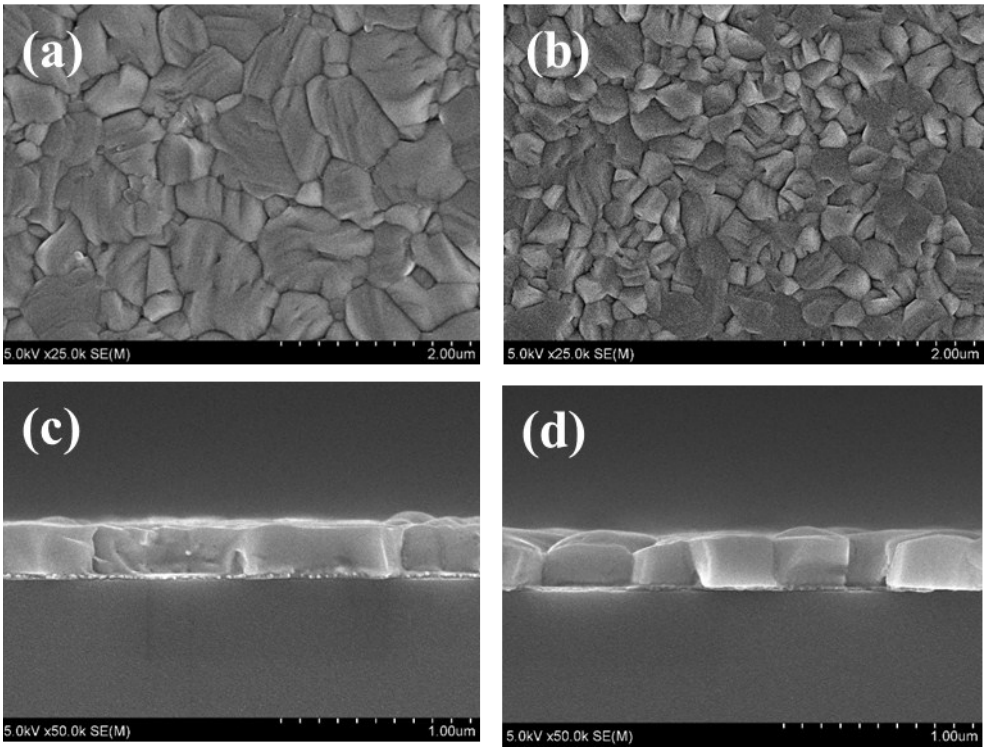

Figure S5. Top view SEM image of perovskite thin film prepared on glass substrate with (a) PTAA (b) PEDOT:PSS and cross-sectional image of respective perovskite films (c,d). Here, surface texture of perovskite film on PTAA shows larger grain size with wide and well grown cross-sectional texture.

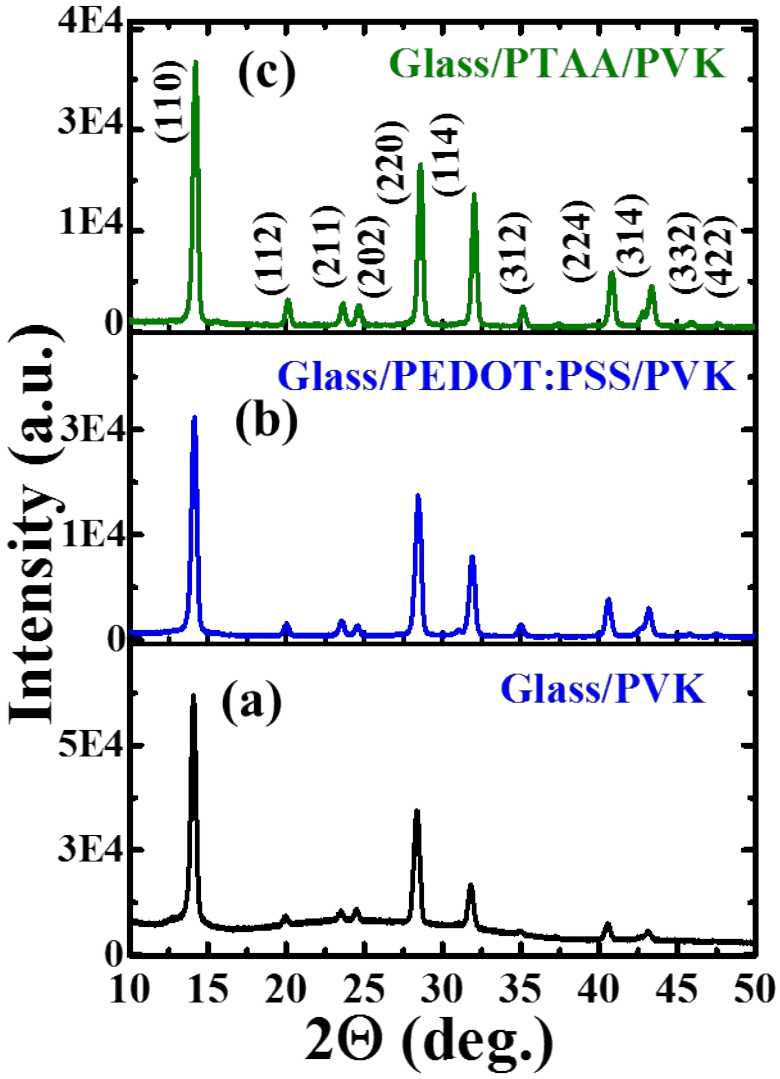

Figure S6. XRD patterns of perovskite (PVK) thin films (a) glass/PVK (b) glass/PEDOT:PSS/PVK (c) glass/PTAA/PVK. All characteristics peaks belong to perovskite crystal. [1-3] Here, PVK on PTAA showed a slightly higher intensity of dominant (110) peak with noticeably enhancement of others characteristic peaks of perovskite crystal inferring improvement in crystal quality.[2,3]

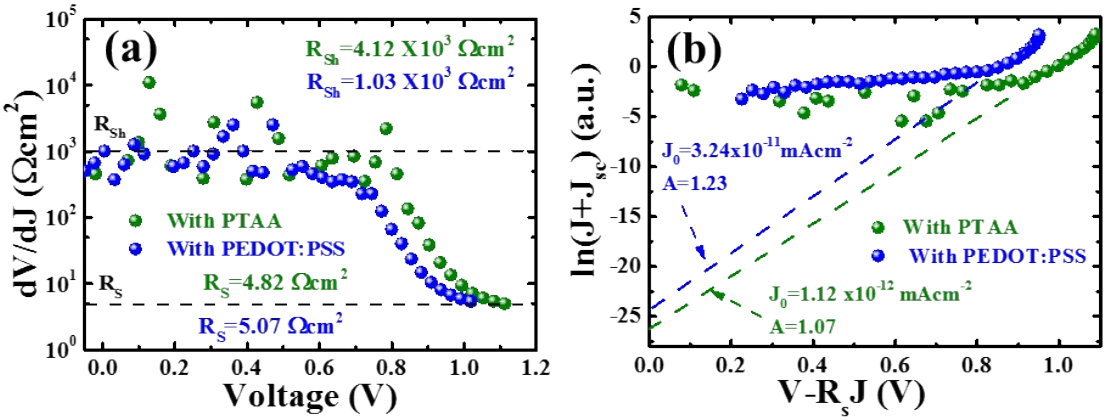

Figure S7. Plots of analysis of J-V characteristics of perovskite devices with PTAA and PEDOT:PSS as HTL for the estimation of characteristics electric properties; series resistance (R_S), shunt resistance (R_{Sh}), diode ideality factor (A) and reverse saturation current (J_0).

Table S2. Calculated electronic properties of the respective devices

Parameters	With PTAA	With PEDOT:PSS
R_s(Ωcm^{-2})	4.82	5.07
R_{sh}(Ωcm^{-2})	4.12x10^3	1.03x10^3
A	1.07	1.23
J_0(mAcm^{-2})	1.12 × 10^{-12}	3.24 × 10^{-11}

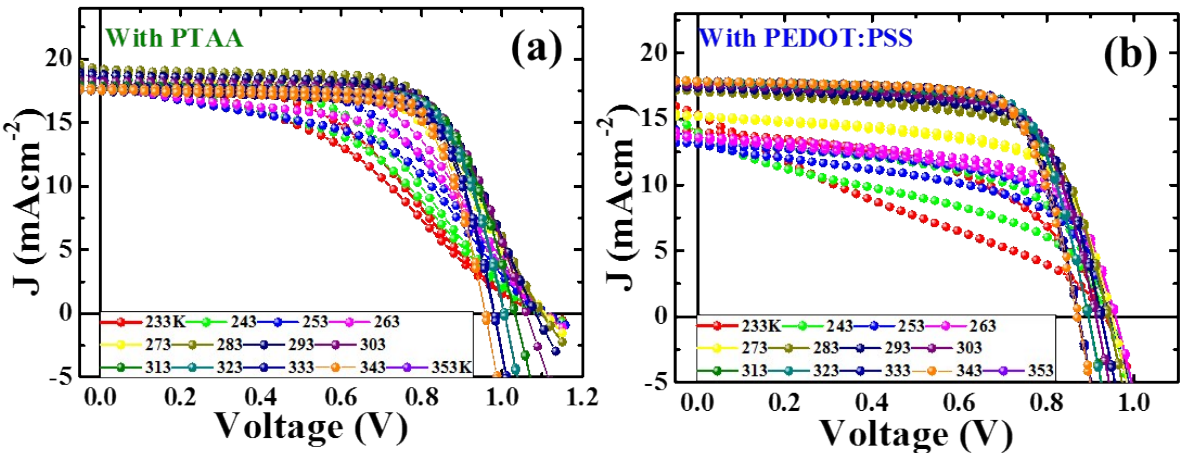

Figure S8. J-V-T characteristic of perovskite devices with PTAA (a) and PEDOT:PSS (b) as HTL.

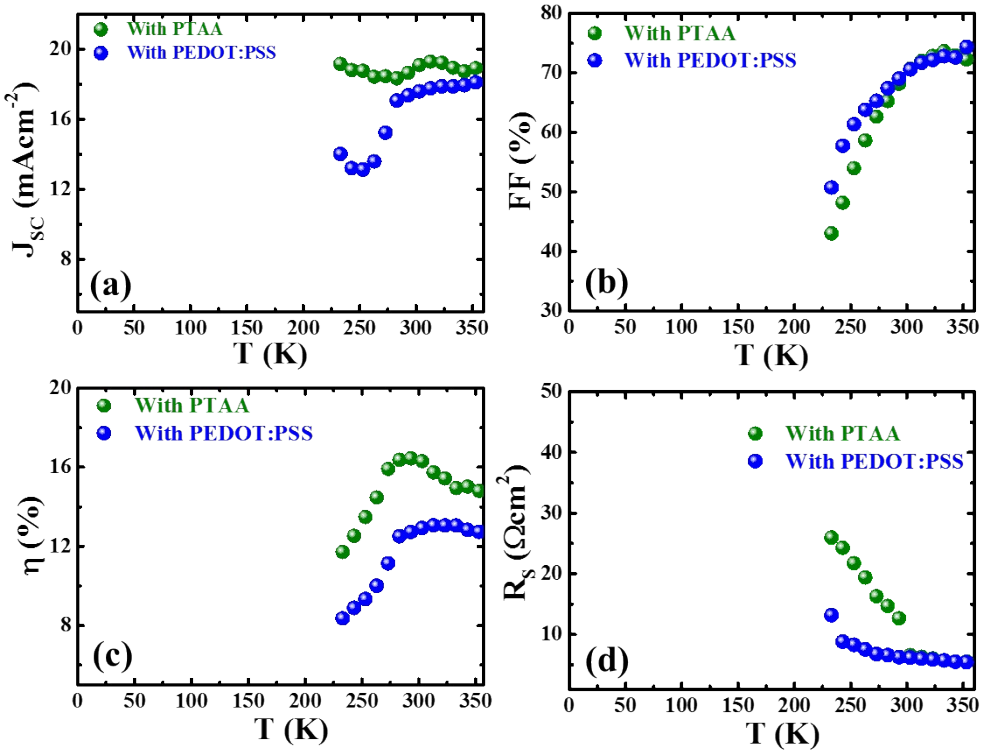

Figure S9. Temperature dependent device parameters of perovskite devices with PTAA and PEDOT:PSS as HTL.

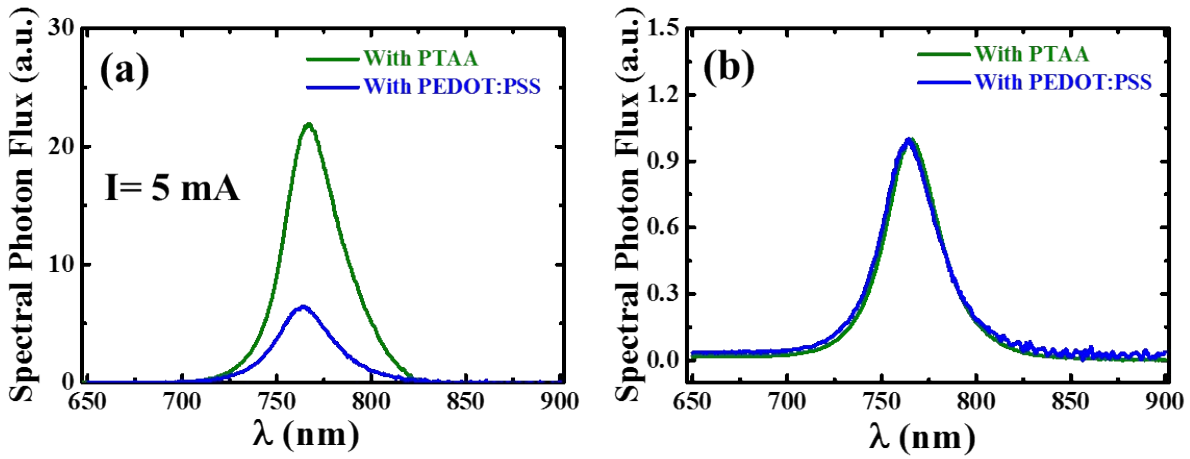

Figure S10. Electroluminescence (EL) spectra (Spectral photon flux) of device with PTAA and PEDOT:PSS (a) and normalized EL spectra of corresponding devices (b).

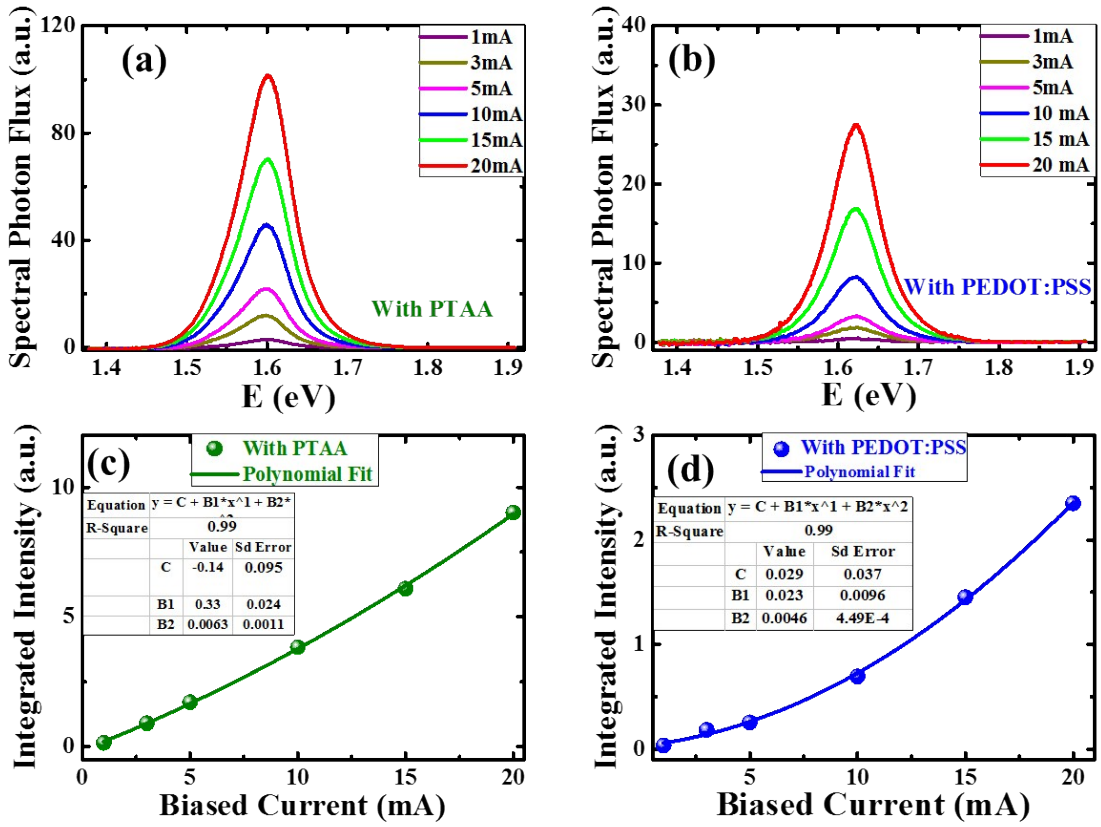

Figure S11. Electroluminescence (EL) spectra of devices with PTAA (a) and PEDOT:PSS (b) under various biased current. The integrated spectral photon flux (EL spectra) with polynomial fit (c, d) of respective devices.

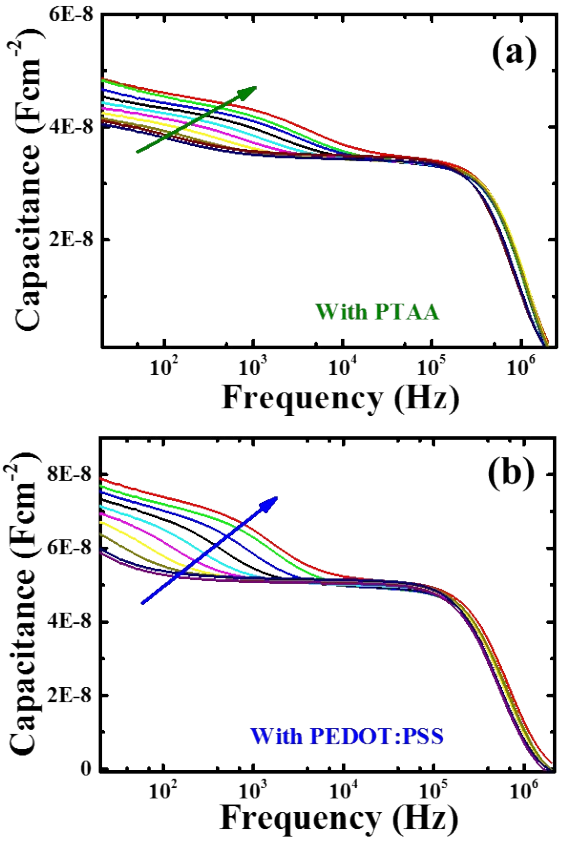

Figure S12. Capacitance frequency (C-f) scans of the devices: with PTAA (a) and PEDOT:PSS (b) in temperature range 243 to 353 K.

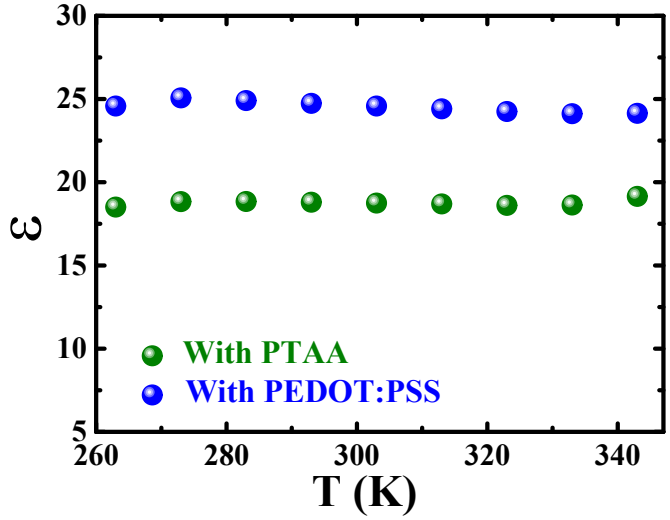

Figure S13. Dielectric constant of perovskite films extracted from analysis of C-f –T scans of respective devices (**Figure 12 a,b**).

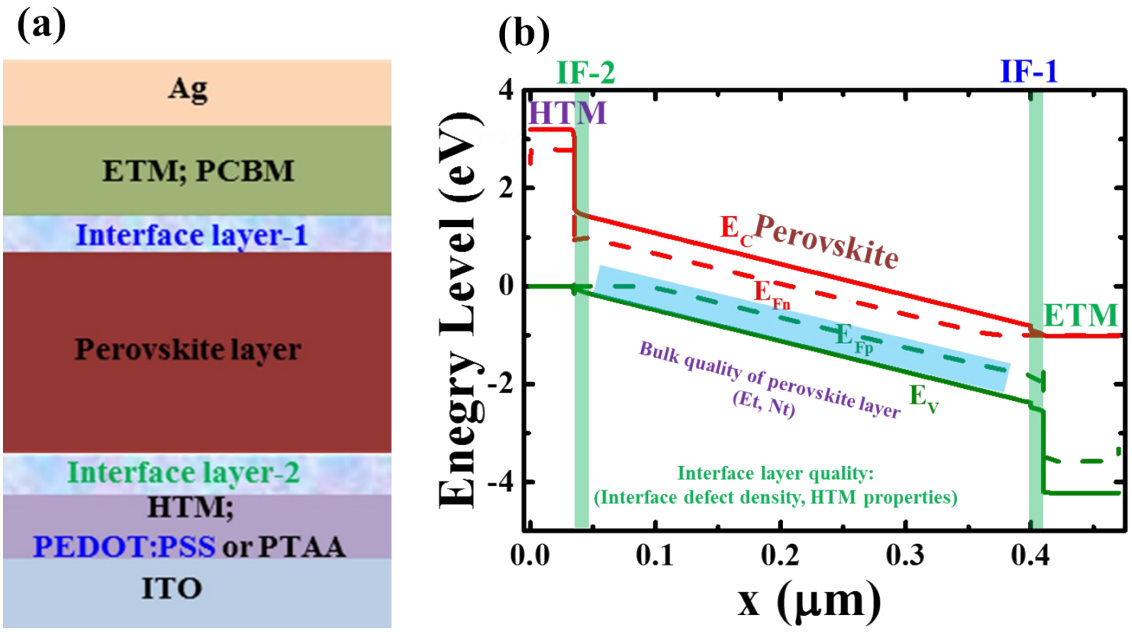

Figure S14. Schematic diagram of device layers defined for SCAPS simulation (a). The simulated energy band (EB) of device as of defined parameters (b). The shadow area indicates area of interest. The device layers were defined (as summarized in Table S3) adopting our earlier report [3] and similar kind of solar cell.[4,5] (HTM: hole transport material, ETM: electron transport material, and IF: interface layer.)

Table S3. Summary of simulation parameters of perovskite solar cell devices for SCAPS simulation. The device layers were defined considering our earlier report [3] and similar kind of solar cell. [4,5] (HTM: hole transport material, ETM: electron transport material, and IF: interface layer.)

Material /Properties	HTM	IF-2	Perovskite	IF-1	ETM
X(μm)	0.035	0.015	0.350	0.010	0.060
E_g (eV)	3.2	1.55	1.55	1.55	3.2
χ(eV)	2.45	3.9	3.9	3.9	4.0
ε_r	3	22	22	22	3
Nc (cm^{-3})	2.2×10^{18}	2.2×10^{18}	2.2×10^{18}	2.2×10^{18}	2.2×10^{18}
Nv (cm^{-3})	1.8×10^{19}	1.8×10^{19}	1.8×10^{19}	1.8×10^{19}	1.8×10^{19}
v_n (cms^{-1})	1×10^{7}	1×10^{7}	1×10^{7}	1×10^{7}	1×10^{7}
v_h (cms^{-1})	1×10^{7}	1×10^{7}	1×10^{7}	1×10^{7}	1×10^{7}
μ_n/μ_h ($cm^2V^{-1}s^{-1}$)	$5\times10^{-4}/5\times10^{-4}$	2/2	4/4	2/2	$5\times10^{-4}/5\times10^{-4}$
N_d(cm^{-3})	-	1×10^{14}	1×10^{14}	1×10^{14}	5×10^{18}
N_a(cm^{-3})	1×10^{19}	1×10^{14}	1×10^{14}	1×10^{14}	-
N_t (cm^{-3})	1×10^{16}	1×10^{14}-1×10^{19}	1×10^{14} - 8×10^{15}	1×10^{14}-1×10^{19}	1×10^{16}
CC of e/h (cm^2)	$5\times10^{-14}/5\times10^{-14}$	$5\times10^{-14}/5\times10^{-14}$	$2\times10^{-14}/2\times10^{-14}$	$5\times10^{-14}/5\times10^{-14}$	$5\times10^{-14}/5\times10^{-14}$
E_t (eV)/distribution	0.5/ Gau	0.4/ Gau	(0.1-0.7)/ Gau	0.4/ Gau	0.5/ Gau
Interface; CC (cm^2)/E_t(eV)/Nt (cm^{-3})	HTM/IF-2; $1\times10^{-14}/0.8/1\times10^{18}$			ETM/IF-1 $1\times10^{-14}/0.8/1\times10^{18}$	

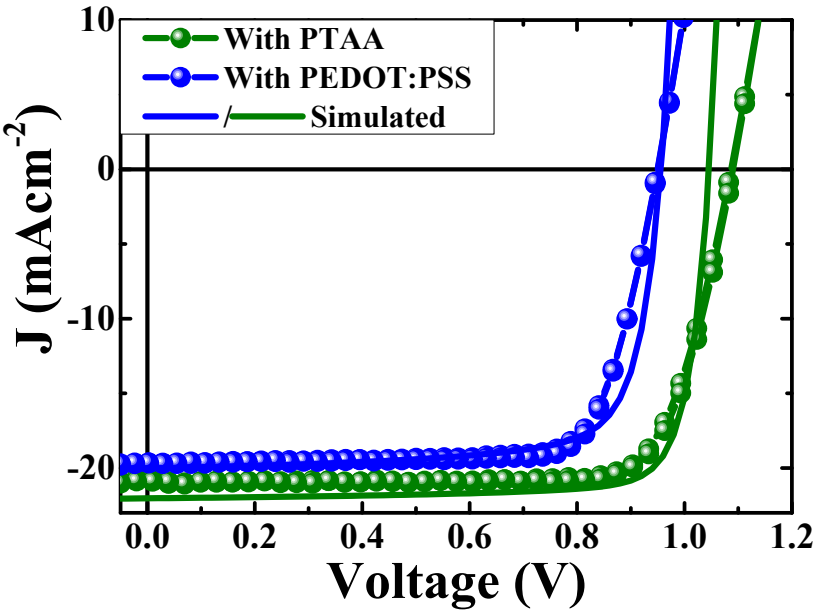

Figure S15. Current density–voltage (J-V) characteristics of devices with PTAA and PEDOT:PSS as HTLs, (**Figure 2a**) and those from simulation. The simulated J-V results were obtained by device simulation using defect levels (E_t)~0.27 and 0.45 eV for device with PEDOT:PSS and ~0.15 and 0.32 eV for device with PTAA, estimated from C-f-T analysis. The bulk defect density in perovskite was assumed to be ~10^{16} cm^{-3} eV^{-1} for the PEDOT:PSS device and slightly lower for PTAA device adopting the trend of the experimental results. Similarly, the interface layer quality induced by HTL is considered by tuning interface defect density in the range 5×10^{18}-1×10^{17} cm^{-3}. These values are within the acceptable range of calculated the experiment data. Other parameters are the same as summarized in **Table S4.**

Table S4. Summary of the device parameters obtained from experiment and simulation.

Device type/ Device parameter	With PEDOT:PSS		With PTAA	
	Experimental	Simulated	Experimental	Simulated
Voc(V)	19.66	20.02	21.01	22.02
Jsc($mAcm^{-2}$)	0.95	0.96	1.09	1.04
FF (%)	0.78	0.76	0.79	0.81
η (%)	14.51	14.47	18.02	18.49

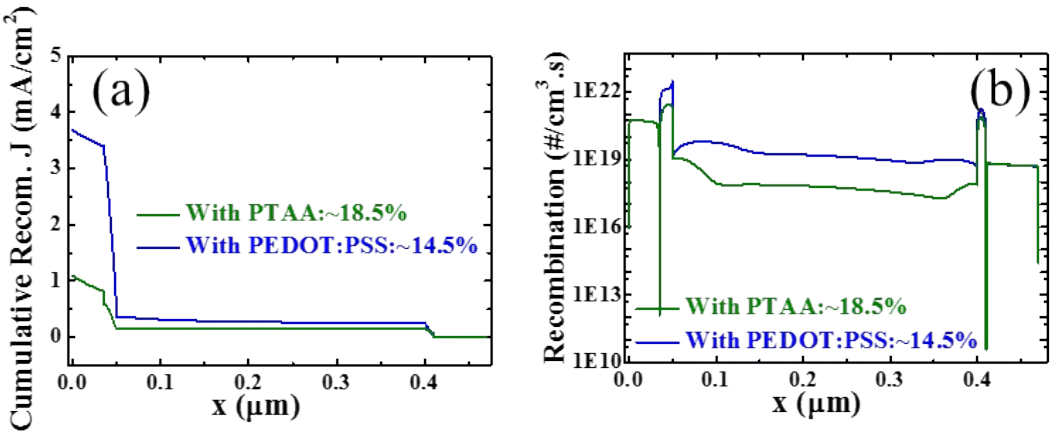

Figure S16. Simulated results of cumulative recombination current (a) and recombination carrier density (b) of respective devices with defined parameters corresponding to simulated J-V data (**Figure S15**). Note that the cumulative recombination current and cumulative recombination density of carriers is lower for the device with PTAA. The lower recombination current and recombination density at interface region (**Figure a, b**) correlate to improvement in interface layer quality in PTAA device.

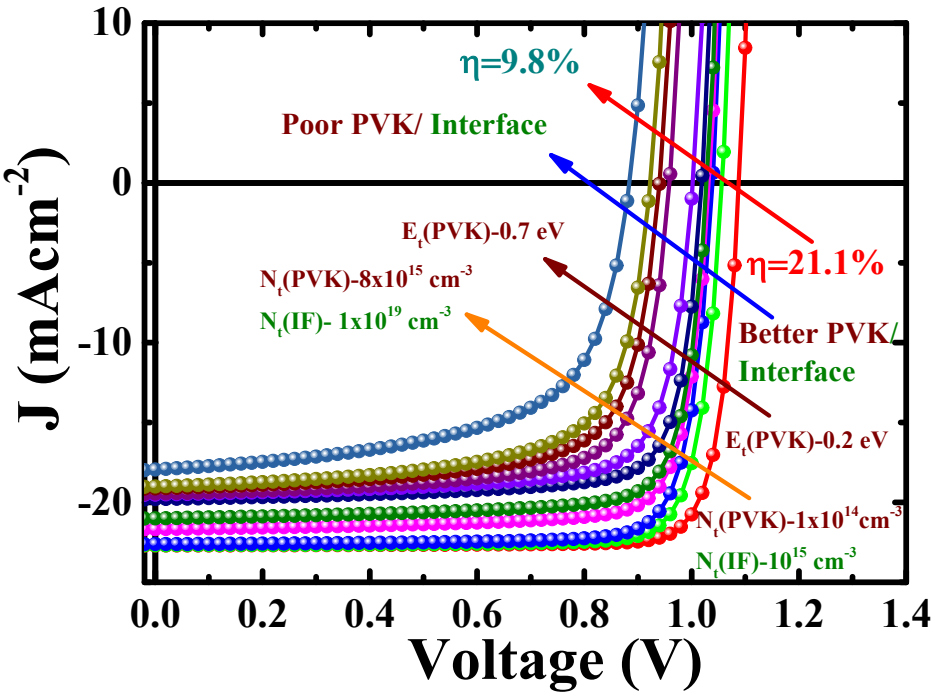

Figure S17. Simulation results showing impact on J-V curves accounting the quality of perovskite (PVK) thin film and interface layer between PVK and carrier transport layers (CTLs). Here, we considered quality of perovskite layer with variation of defect density (N_t (PVK); $1x10^{14}$ to $8x10^{15}$ cm^{-3}) and defect level (E_t; 0.2 to 0.7 eV) in bulk of perovskite layer and interface layer quality was accounted by varying the defect density at interface (IF) layer (Nt (IF); $1x10^{15}$ to $1x10^{19}$ cm^{-3}) as depicted in plot. Other non-varied parameters were taken same as summarized in Table S3. The simulated results revealed a correlative trend of decrease in device performance with increase in values of Nt (PVK), Et and Nt (IF).

References

[1] M. I. Saidaminov, A. L. Abdelhady, B. Murali, E. Alarousu, V. M. Burlakov, W. Peng, I. Dursun, L. Wang, Y. He, G. Maculan, A. Goriely, T. Wu, O. F. Mohammed and O. M. Bakr, High-quality bulk hybrid perovskite single crystals within minutes by inverse temperature crystallization, Nat. Commun., 2015, 6, 7586.

[2] H. P. Zhou, Z. R. Hong, S. Luo, H. S. Duan, H. H. Wang, Y. S. Liu, G. Li and Y. Yang, Planar Heterojunction Perovskite Solar Cells via Vapor-Assisted Solution Process, Q. Chen, J. Am. Chem. Soc., 2014, 136, 622–625.

[3] D. B. Khadka, Y. Shirai, M. Yanagida, T. Masuda, K. Miyano, Enhancement in Efficiency and Optoelectronic Quality of Perovskite thin films Following MACl Ambient Annealing, *Sustainable Energy and Fuels,* **2017**, 1, 755-766

[4] F. Liu, J. Zhu, J. Wei, Y. Li, M. Lv, S. Yang, B. Zhang, J. Yao, S. Dai, Numerical Simulation: Toward the Design of High-Efficiency Planar Perovskite Solar Cells, *Appl. Phys. Lett.* **2014**, 04, 253508.

[5] T. Minemoto, M. Murata, Device Modeling of Perovskite Solar Cells Based on Structural Similarity with Thin Film Inorganic Semiconductor Solar Cells, *J. Appl. Phys.* **2014**, 116, 054505.